

Reflectivity of a Cholesteric Liquid Crystal

A Senior Project

presented to

the Faculty of the Physics Department

California Polytechnic State University, San Luis Obispo

In Partial Fulfillment

of the Requirements for the Degree

Bachelor of Science

by

Justin Lawson

January, 2010

© 2010 Justin Lawson

Introduction:

A cholesteric liquid crystal is one in which the director \mathbf{n} rotates as one proceeds orthogonally between layers of approximately constant \mathbf{n} . This paper will assume the director rotates in the xy plane and changes orientation as a function of z. Generally the director is given by

$$\mathbf{n} = \cos\phi(z)\hat{x} + \sin\phi(z)\hat{y} \quad (1)$$

where $\phi(z)$ is the angle between the director and the x axis. This paper will focus predominantly on the simple case where $\phi(z)$ is linearly dependent on z, that is

$$\phi(z) = \frac{2\pi}{P}z = q_0z \quad (2)$$

Here P is the repeat distance or pitch of the cholesteric. The calculations from the first section parallel those from chapter 6 of de Gennes' The Physics of Liquid Crystals (that work should be used as a supplement to the following material) and discusses solutions to the wave equation

$$\frac{\partial^2}{\partial z^2} \vec{\mathbf{E}} = \frac{1}{c^2} \frac{\partial^2}{\partial t^2} \vec{\mathbf{D}} \quad (3)$$

inside a cholesteric liquid crystal of constant pitch (where $\mathbf{D} = \hat{\epsilon}\mathbf{E}$ and $\hat{\epsilon}$ is a tensor). In the second section, I solve numerically for the reflection coefficient by solving a boundary condition problem between a vacuum and the chiral liquid crystal for finite width and infinitely long crystals. The third section discusses briefly a few features of the varying pitch case.

Section 1:

From equation (3), the total electric field will have the form

$$\vec{\mathbf{E}}(\vec{r}, t) = E_x(z, t)\hat{i} + E_y(z, t)\hat{j} \quad (1.1)$$

In order to solve the wave equation (3) de Gennes introduces the following change of variables to circular amplitudes

$$E_+ = E_x + iE_y \quad E_- = E_x - iE_y \quad (1.2)$$

To see why these might be considered circular wave amplitudes consider a solution in the +/- plane that remains on the + axis, that is $E_- = 0$. Then $E_x = iE_y$. First let us assume a time dependence of $e^{i\omega t}$ for the field which will simplify the wave equation to an ODE (having only one (spatial) variable) as follows:

$$-\frac{d^2}{dz^2}\vec{E} = \left(\frac{\omega}{c}\right)^2 \hat{\epsilon}(z)\vec{E} \quad (1.3)$$

where $\hat{\epsilon}(z)$ is the dielectric tensor changing as the director rotates. At a fixed z (say z_0) E_x will have the form $E_x(z_0, t) = Ae^{i\omega t}$. Then along the $+$ axis E_y will be given by

$$E_y = -iAe^{i\omega t} = Ae^{i(\omega t - \frac{\pi}{2})} \quad (1.4)$$

Taking real parts we have $\text{Re}(E_x) = A\cos(\omega t)$ and $\text{Re}(E_y) = A\sin(\omega t)$ which is the equation for a circle of radius A rotating counterclockwise in the xy -plane. $E_+ = 2Ae^{i\omega t}$ and $\text{Re}(E_+) = 2A\cos(\omega t)$ in this case. Figure 1.1 below shows the same function in both the $+/ -$ and xy planes a linearly polarized field on the $+$ axis is right circularly polarized field in the xy plane.

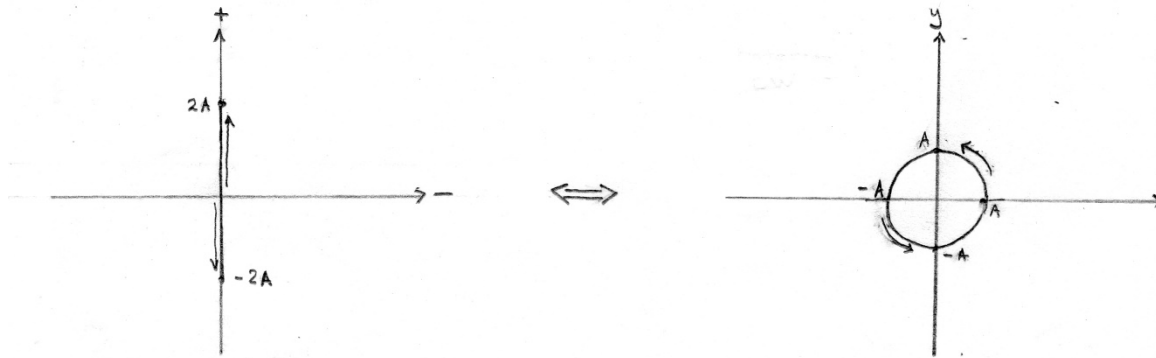


Figure 1.1

A similar argument shows that when a function oscillates along the $-$ axis ($E_+ = 0$) it represents a left circularly polarized field in the xy -plane. In general, solutions to the wave equation may not lie on either the $+$ or $-$ axis but will have components along each which correspond to having perfectly CW and CCW circularly polarized components in the xy -plane. Adding left and right circularly polarized components in the xy -plane will generally yield elliptically polarized solutions (see Figure 1.2 below).

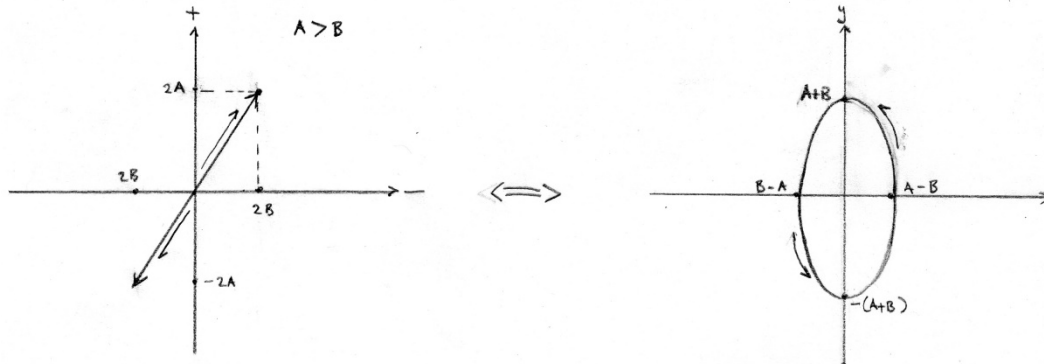


Figure 1.2

Generally, whichever field amplitude, A or B, is larger will determine the direction of rotation. For example in Figure 1.2, $A > B$ ($E_+ > E_-$) and the corresponding ellipse precesses in a counterclockwise direction. The +/- plane can be broken up as shown in Figure 1.3 according to this relationship.

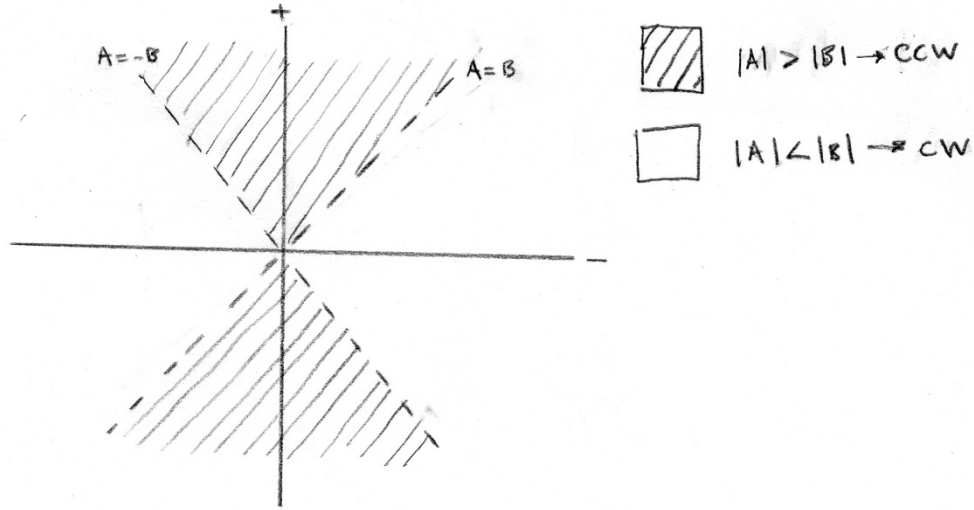


Figure 1.3

In the case of linear z dependence, the dielectric tensor $\hat{\epsilon}(z)$ is given by

$$\hat{\epsilon}(z) = \frac{\epsilon_1 + \epsilon_2}{2} \begin{pmatrix} 1 & 0 \\ 0 & 1 \end{pmatrix} + \frac{\epsilon_1 - \epsilon_2}{2} \begin{pmatrix} \cos 2q_0 z & \sin 2q_0 z \\ \sin 2q_0 z & -\cos 2q_0 z \end{pmatrix} \quad (1.5)$$

Here ϵ_1 is the dielectric constant parallel to the director and ϵ_2 is that orthogonal to the director. Using (1.5) and (1.2) in the wave equation (1.3) yields

$$\frac{-d^2 E^+}{dz^2} = k_0^2 E^+ + k_1^2 \exp(2iq_0 z) E^- \quad (1.6a)$$

$$\frac{-d^2 E^-}{dz^2} = k_1^2 \exp(-2iq_0 z) E^+ + k_0^2 E^- \quad (1.6b)$$

where

$$k_0^2 = \left(\frac{\omega}{c} \right)^2 \frac{\epsilon_1 + \epsilon_2}{2} \quad k_1^2 = \left(\frac{\omega}{c} \right)^2 \frac{\epsilon_1 - \epsilon_2}{2} \quad (1.7)$$

The solutions to the coupled set of equations (1.6a/b) are as follows (this and the derivation of $\hat{\epsilon}(z)$ are carried out in more depth in de Gennes')

$$E_+ = a \exp\{i(l + q_0)z\} \quad E_- = b \exp\{i(l - q_0)z\} \quad (1.8)$$

From (1.2) we may now rewrite E_x and E_y in terms of E_+ and E_-

$$E_x = \frac{E_+ + E_-}{2} \quad E_y = \frac{E_+ - E_-}{2i} \quad (1.9)$$

Substituting these into (1.8) then gives

$$\begin{aligned} E_x &= e^{ilz} [ae^{iq_0z} + be^{-iq_0z}] = e^{ilz} [(a+b) \cos q_0z + i(a-b) \sin q_0z] \\ E_y &= e^{ilz} [-i(ae^{iq_0z} - be^{-iq_0z})] = e^{ilz} [-i(a-b) \cos q_0z + (a+b) \sin q_0z] \end{aligned} \quad (1.10)$$

Let $a + b = \zeta$ and $a - b = \rho$. Also we reintroduce the time component into E_x and E_y (multiply by $e^{i\omega t}$); we now write E_{xt} and E_{yt} which are just $E_x(z,t)$ and $E_y(z,t)$. Expanding complex exponentials in terms of sine and cosine we have

$$\begin{aligned} E_{xt} &= (\cos \omega t + i \sin \omega t)(\cos lz + i \sin lz)(\zeta \cos q_0z + i\rho \sin q_0z) \\ E_{yt} &= (\cos \omega t + i \sin \omega t)(\cos lz + i \sin lz)(-i\rho \cos q_0z + \zeta \sin q_0z) \end{aligned} \quad (1.11)$$

Taking the real components of E_{xt} and E_{yt} gives

$$\begin{aligned} \text{Re}(E_{xt}) &= \cos \omega t \{ \zeta \cos(q_0z) \cos(lz) - \rho \sin(q_0z) \sin(lz) \} \\ &\quad - \sin \omega t \{ \rho \sin(q_0z) \cos(lz) + \zeta \cos(q_0z) \sin(lz) \} \\ \text{Re}(E_{yt}) &= \cos \omega t \{ \zeta \sin(q_0z) \cos(lz) + \rho \cos(q_0z) \sin(lz) \} \\ &\quad + \sin \omega t \{ \rho \cos(q_0z) \cos(lz) - \zeta \sin(q_0z) \sin(lz) \} \end{aligned} \quad (1.12)$$

If we now rotate into the frame of the director (that is take $\phi = q_0z = 0$ making $\sin(q_0z) = 0$ and $\cos(q_0z) = 1$) such that the x axis is rotated perpendicular to the director axis (call this η) and y is rotated perpendicular to the director (call this axis ξ) we obtain

$$\begin{aligned} \text{Re}(E_\eta) &= \zeta [\cos(\omega t) \cos(lz) - \sin(\omega t) \sin(lz)] \\ \text{Re}(E_\xi) &= \rho [\cos(\omega t) \sin(lz) + \sin(\omega t) \cos(lz)] \end{aligned} \quad (1.13)$$

Letting $\text{Re}(E_\eta) = E_\eta$ and $\text{Re}(E_\xi) = E_\xi$ in the next equation, it can be shown

$$\frac{E_\eta^2}{\zeta^2} + \frac{E_\xi^2}{\rho^2} = 1 \quad (1.14)$$

(1.14) is just the equation for an ellipse with major axis $\zeta = a + b$ and minor axis $\rho = a - b$. Thus the solutions are elliptically polarized in the rotating frame of the cholesteric. From (1.13) we also gather that the field is elliptically “polarized” in z (it traces an ellipse as z changes with angular “frequency” ℓ). This can be seen if we choose a coordinate system which itself rotates with the director (see Warner and Kutter); we would find in that coordinate frame and for a fixed time, the field traced out an ellipse as z changed. The series of pictures in Appendix A are meant to illustrate this behavior (approximate amplitudes from Figure 1.2 are used).

It can be shown (using (1.13) and graphing for $\ell > 0$ the cases ρ & $\zeta > 0$, $\rho > 0$ & $\zeta < 0$, etc. then repeating for $\ell < 0$) that the sign of the axial ratio $\chi = \rho / \zeta$ determines the direction of rotation. For $\chi > 0$ the ellipse rotates counterclockwise and for $\chi < 0$ it rotates clockwise (Appendix B illustrates this).

Furthermore we can show that the inequality $\chi > 0$ is identical to $|a| > |b|$: which we expected from our analysis of the E_+ and E_- solutions in the \pm plane:

$$\begin{aligned} \chi = \frac{a-b}{a+b} > 0 & \quad \rightarrow \quad \frac{a-b}{a+b} + 1 > 1 \quad \rightarrow \quad \frac{a-b}{a+b} + \frac{a+b}{a+b} > \frac{a+b}{a+b} \\ \rightarrow \quad \frac{2a}{a+b} > \frac{a+b}{a+b} & \quad \rightarrow \quad 2a(a+b) > (a+b)^2 \quad \rightarrow \quad 2a^2 > a^2 + b^2 \\ & \quad \rightarrow \quad a^2 > b^2 \equiv |a| > |b| \end{aligned}$$

This reaffirms the conclusion that $|a| > |b|$ corresponds to a counterclockwise rotating (right circularly polarized) ellipse while $|a| < |b|$ corresponds to a clockwise rotating (left circularly polarized) ellipse.

* * *

The coefficients a and b from equation (1.8) are related by the set of equations

$$\begin{aligned} \{(l + q_0)^2 - k_0^2\}a - k_1^2 b &= 0 \\ -k_1^2 a + \{(l - q_0)^2 - k_0^2\}b &= 0 \end{aligned} \tag{1.15}$$

which have non-trivial solutions only if the corresponding determinant vanishes, that is

$$(-k_0^2 + l^2 + q_0^2)^2 - 4q_0^2 l^2 - k_1^4 = 0 \tag{1.16}$$

Substituting the expressions from (1.7) into (1.16) we have a fourth order polynomial and expect four solutions for ω as a function of ℓ . Two of these will be positive (i.e. $\omega(\ell) > 0$ for all ℓ) and two negative (these don't make physical sense). Figure 1.4 below is a hand sketched reproduction of the two positive $\omega(\ell)$'s found by Matlab (they have been named

ω_2 and ω_4 because they are the second and fourth components of the Matlab's vector solution to (1.16)).

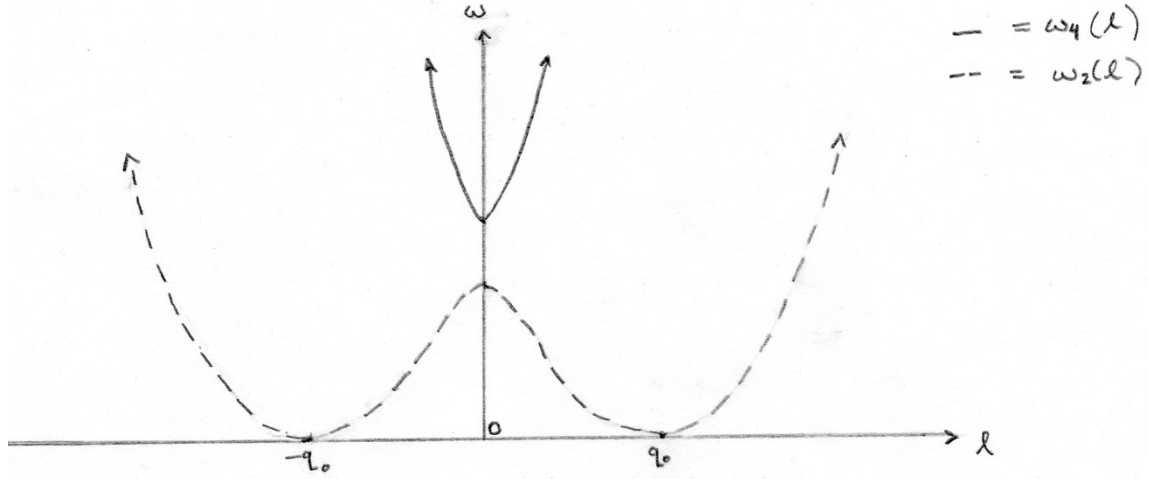


Figure 1.4

From (1.15) we may define a quantity τ given by

$$\tau = a/b = \frac{k_1^2}{(l+q_0)^2 - k_0^2} = \frac{(l-q_0)^2 - k_0^2}{k_1^2} \quad (1.17)$$

Graphing $\tau(\ell)$ again by replacing k_0 and k_1 according to (1.7), we get Figure 1.5. Figure 1.6 is a hand-drawn clarification.

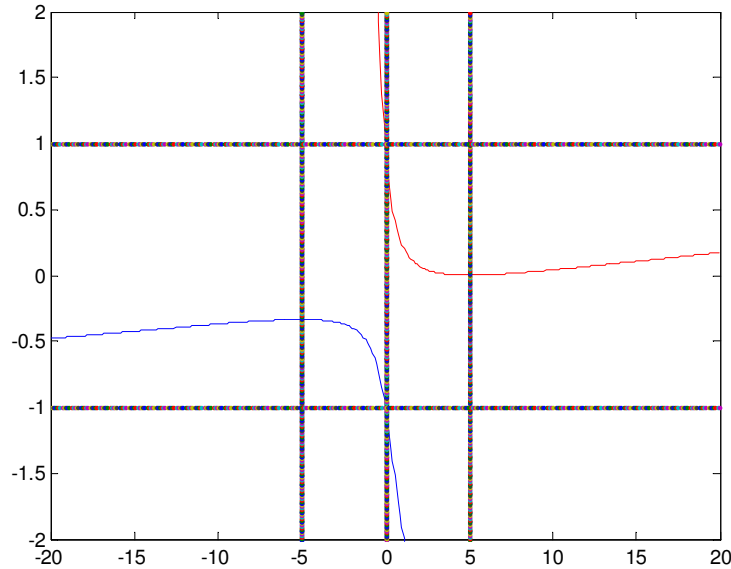


Figure 1.5

The above plot of τ vs. ℓ is drawn again below. Here $q_0=5$ and as $\ell \rightarrow \pm\infty$, $|\tau| \rightarrow 1$ consistent with DeGennes prediction that the electric field is circularly polarized in this limit

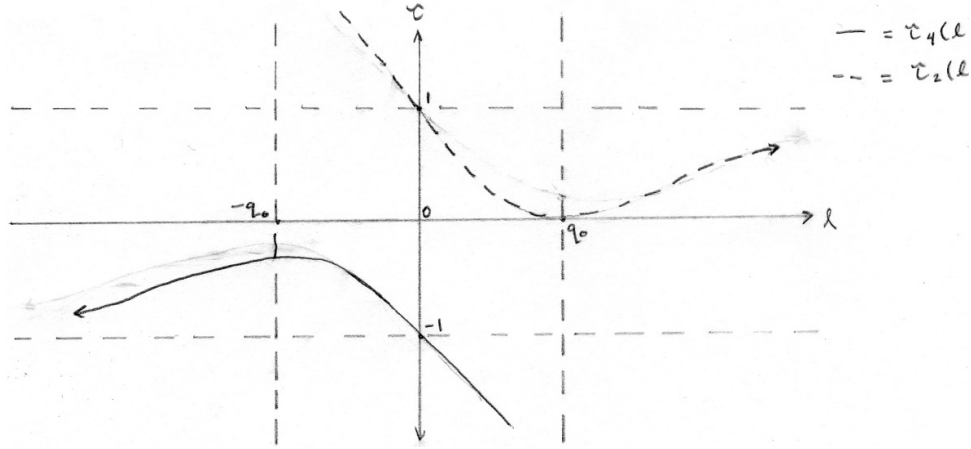


Figure 1.6

Here the dotted function is $\tau_4(\ell)$ where ω_4 (the top parabola in Fig. 1.4) has been used in (1.17) and the solid-line function is $\tau_2(\ell)$ which we got by plugging ω_2 (the bottom W-shaped line in Fig. 1.4) into (1.17).

Comparison with Figure 1.3 tells us that $|\ell| > 1$ corresponds to counterclockwise rotation and $|\ell| < 1$ to clockwise rotation.

From figure 1.4 we know $\omega_2(\pm q_0) = 0$, the respective k -values from equation (1.7) are $k_0(0) = 0$ and $k_1(0) = 0$. Thus by (1.17), $\tau_2(q_0) = 0/(4q_0^2) = 0$ and $\tau_2(-q_0) = (4q_0^2)/0 = \infty$; which Figure 1.6 shows.

Furthermore, $\tau_4(0) = -1$ corresponds to $a = -b$ (at what de Gennes calls ω_+ or the larger of the two solutions to $\omega(0)$) and $\tau_2(0) = 1$ to $a = b$ (at his ω_- the smaller of the two). These represent linearly polarized waves parallel and perpendicular, respectively, to the director. We also expect for $\ell = \pm q_0$ that the wave will be circularly polarized (either a or b will be zero and τ_2 will equal 0 or ∞ respectively).

The region $-1 < \tau < 1$ corresponds to $|a| < |b|$ and $-1 > \tau > 1$ to $|a| > |b|$ (left and right circularly polarized ellipses respectively). This is summarized by Figure 1.7 below.

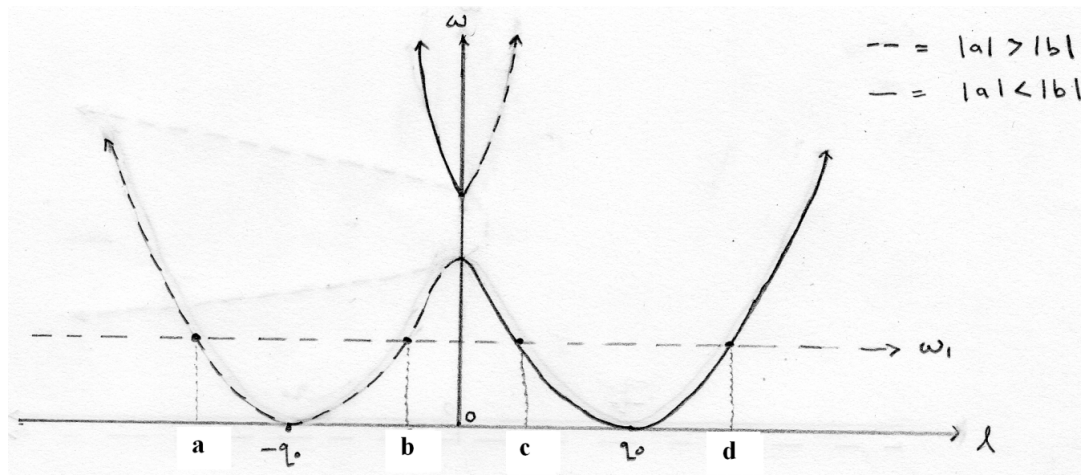


Figure 1.7

The rest of this paper will use the convention $\ell_a < \ell_b < \ell_c < \ell_d$ outside of the gap.

Outside the gap there will be four ℓ values for any given frequency including two forward and two backward traveling solutions. The forward traveling solutions are those with a positive group velocity (for which $d\omega/d\ell > 0$) and the backward traveling solutions those with a negative group velocity ($d\omega/d\ell < 0$). For the pair of forward travelling solutions (not in the gap) we can also state using Figure 1.7 that one will precess clockwise and the other counterclockwise in the xy plane (the same holds for the pair of backward traveling solutions). For example, at ω_1 , the forward travelling solution ℓ_b corresponds to a counterclockwise precessing ellipse and the forward travelling solution ℓ_d corresponds to a clockwise precessing ellipse.

In the frequency gap, there will only be two real solutions for ℓ (one forward and one backward travelling) the other two solutions will be imaginary. To see this we plot both $\omega(\ell)$ and $\omega(\ell^2)$ on the same graph (Figure 1.8 below is the Matlab version, Figure 1.9 the clarified hand-drawn version).

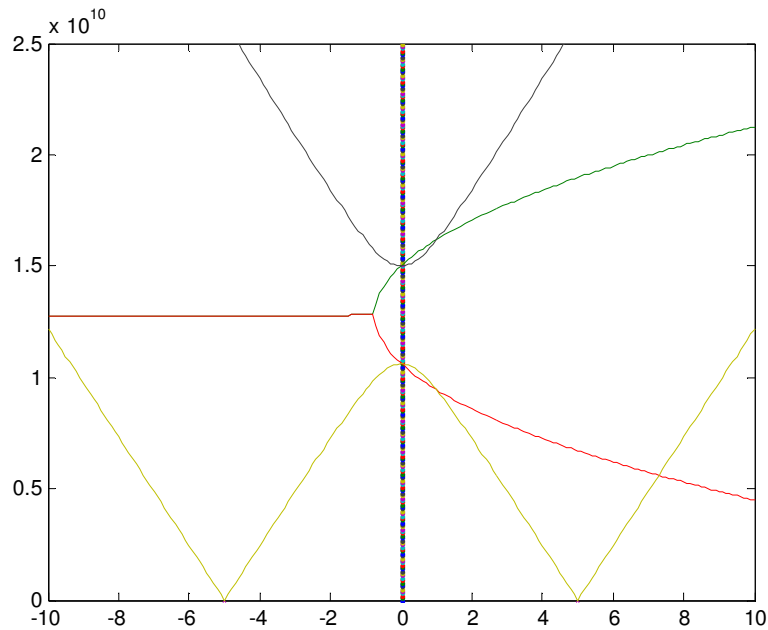


Figure 1.8
Plot of ω vs. ℓ and ω vs. ℓ^2 . See clarification below.

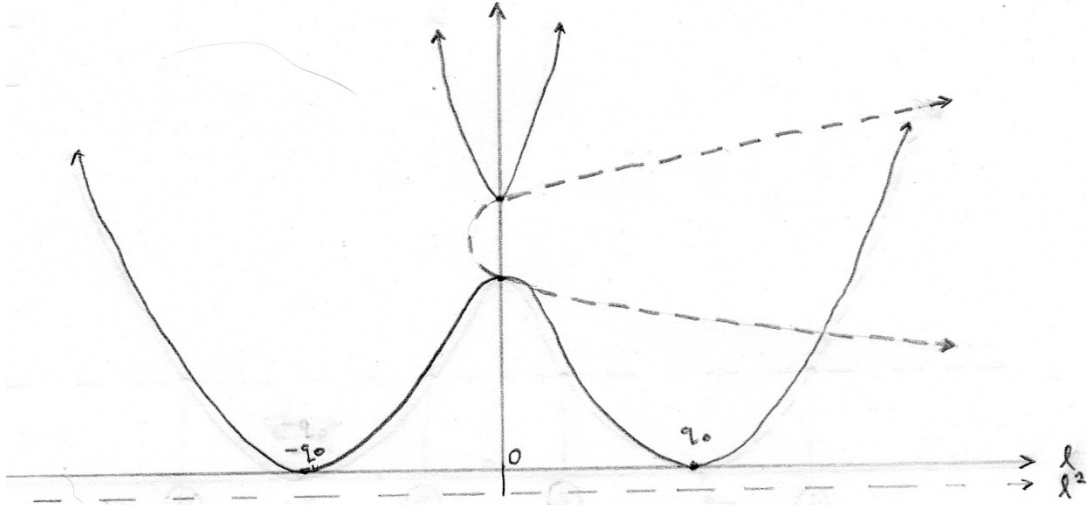


Figure 1.9 (shape poorly drawn but points of contact are accurate)

As can be seen solutions to ℓ^2 become negative in the frequency gap corresponding to imaginary values of ℓ . These in turn represent decaying or expanding field solutions in the gap (see equation (1.8): if ℓ is imaginary, an exponential with a real argument can be factored out of E_+ and E_-). In the gap we expect the field to attenuate as it travels. By inspecting equation (1.8) it can be seen that the positive imaginary root of ℓ^2 will correspond to the forward traveling wave (since the field decays from left to right) and the negative root to the backwards traveling wave (since it decays oppositely).¹

Section 2:

In this section we consider the solutions to the wave equation at the boundary between the crystal and a medium with a constant ϵ (not dependent on a director position). Taking the z direction to be perpendicular to the plane of incidence the boundary conditions on the electro-magnetic field (for a boundary which has no free surface current) are:

$$\vec{E}_1^{\parallel} - \vec{E}_2^{\parallel} = 0 \quad \text{and} \quad \frac{1}{\mu_1} \vec{B}_1^{\parallel} - \frac{1}{\mu_2} \vec{B}_2^{\parallel} = 0 \quad (2.1a) \text{ \& } (2.1b)$$

(here the subscripts 1 and 2 denote the different media). Since we would like to deal only with the electric field (this is what we have an expression for, (1.8) above) we can rewrite the second condition using one of Maxwell's equations,

¹ The reader may here wonder why there only appears to be one ℓ^2 value for a given ω . There is actually another branch of the $\omega(\ell^2)$ solution which intersects the ℓ^2 axis at q_0^2 but just does not appear in the range of the above graphs.

$$\nabla \times \vec{E} = -\frac{d\vec{B}}{dt} \quad (2.2)$$

we had already assumed a time dependence proportional to $e^{-i\omega t}$ which gives us

$$\left(\frac{\partial E_z}{\partial y} - \frac{\partial E_y}{\partial z}\right)\hat{i} - \left(\frac{\partial E_z}{\partial x} - \frac{\partial E_x}{\partial z}\right)\hat{j} + \left(\frac{\partial E_y}{\partial x} - \frac{\partial E_x}{\partial y}\right)\hat{k} = i\omega\vec{B} \quad (2.3)$$

but since we are considering a wave polarized perpendicular to the boundary (normal incidence), $E_z = 0$ and the second condition, equation (2.1b), becomes:

$$\frac{1}{\mu_1} \frac{\partial}{\partial z} \vec{E}_1^{\parallel} - \frac{1}{\mu_2} \frac{\partial}{\partial z} \vec{E}_2^{\parallel} = 0 \quad (2.4)$$

Thus our set of boundary conditions in terms of the electric field is given by:

$$\vec{E}_1^{\parallel} - \vec{E}_2^{\parallel} = 0 \quad (2.5a)$$

$$\frac{1}{\mu_1} \frac{\partial}{\partial z} \vec{E}_1^{\parallel} - \frac{1}{\mu_2} \frac{\partial}{\partial z} \vec{E}_2^{\parallel} = 0 \quad (2.5b)$$

We now consider, an incident wave, polarized normal to the boundary, in $\pm z$ space defined by (1.3) whose general form will be:

$$E_{i+} = a_i e^{i\kappa z} \quad \text{and} \quad E_{i-} = b_i e^{i\kappa z} \quad (2.6)$$

where $\kappa = \omega n/c$ is just constant in the first medium. The reflected wave will have a similar form only with a negative κ to indicate that the wave is traveling in the opposite (negative z) direction:

$$E_{r+} = a_r e^{-i\kappa z} \quad \text{and} \quad E_{r-} = b_r e^{-i\kappa z} \quad (2.7)$$

The transmitted wave, traveling in the cholesteric, has the solutions given by (1.8) above. Incorporating both forward traveling modes (corresponding to different l values) into a single expression we have

$$E_{t+} = a_{t1} e^{i(l_1+q_0)z} + a_{t2} e^{i(l_2+q_0)z} \quad (2.8a)$$

$$E_{t-} = b_{t1} e^{i(l_1-q_0)z} + b_{t2} e^{i(l_2-q_0)z} \quad (2.8b)$$

(Here the subscripts 1 and 2 denote the different modes within the crystal or different solutions to (1.16), instead of the medium). Since this wave is forward traveling, the group velocity must be positive so l_1 and l_2 are those solutions for which $\partial\omega/\partial l > 0$ in Figure 1.7. Below the gap ($\omega < \omega^-$) $l_1 = l_d$ and $l_2 = l_b$. Above the gap ($\omega > \omega^+$) $l_1 = l_d$ and $l_2 = l_c$. Inside the gap l_1 is still equal to l_d and l_2 will be equal to the positive imaginary root of the l^2 function plotted in Figures 1.8 and 1.9.

Applying condition (2.5a) at the boundary where $z = 0$ to (2.6), (2.7) and (2.8a/b), we have

$$a_i + a_r = a_{t1} + a_{t2} \quad (2.9a)$$

$$b_i + b_r = b_{t1} + b_{t2} \quad (2.9b)$$

Applying condition (2.5b) at the boundary we obtain

$$\frac{1}{\mu_1} [\kappa a_i - \kappa a_r] = \frac{1}{\mu_2} [(l_1 + q_0) a_{t1} + (l_2 + q_0) a_{t2}] \quad (2.10a)$$

$$\frac{1}{\mu_1} [\kappa b_i - \kappa b_r] = \frac{1}{\mu_2} [(l_1 - q_0) b_{t1} + (l_2 - q_0) b_{t2}] \quad (2.10b)$$

From (1.15) there are the further constraints:

$$a_{t1} = \frac{k_1^2 b_{t1}}{(l_1 + q_0)^2 - k_0^2} = \alpha_1 b_{t1} \quad (2.11a)$$

$$a_{t2} = \frac{k_1^2 b_{t2}}{(l_2 + q_0)^2 - k_0^2} = \alpha_2 b_{t2} \quad (2.11b)$$

(The decision to use α_1 and α_2 here instead of τ_2 and τ_4 as (1.17) would suggest is an attempt to avoid subscript confusion. Concerning α , the subscript is a reference to the mode we are considering).

In the above system of equations, as in experiment, we are free to determine the incident amplitudes a_i and b_i . This leaves us with six equations and six unknown amplitudes (a_r , a_{t1} , a_{t2} , b_r , b_{t1} , and b_{t2}). Using equations (2.11a) and (2.11b) above we can get rid of a_{t1} and a_{t2} in equations (2.9a/b) and (2.10a/b). Equations (2.9a/b) can be rewritten as

$$a_r = \alpha_1 b_{t1} + \alpha_2 b_{t2} - a_i \quad (2.12a)$$

$$b_r = b_{t1} + b_{t2} - b_i \quad (2.12b)$$

and substituting into (2.10a/b) then yields

$$\frac{2\kappa a_i}{\mu_1} = \left[\frac{\kappa}{\mu_1} + \frac{(l_1 + q_0)}{\mu_2} \right] \alpha_1 b_{t1} + \left[\frac{\kappa}{\mu_1} + \frac{(l_2 + q_0)}{\mu_2} \right] \alpha_2 b_{t2} \quad (2.13a)$$

$$\frac{2\kappa b_i}{\mu_1} = \left[\frac{\kappa}{\mu_1} + \frac{(l_1 - q_0)}{\mu_2} \right] b_{t1} + \left[\frac{\kappa}{\mu_1} + \frac{(l_2 - q_0)}{\mu_2} \right] b_{t2} \quad (2.13b)$$

This can in turn be written in the matrix form

$$\begin{bmatrix} \left[\frac{\kappa}{\mu_1} + \frac{(l_1 + q_0)}{\mu_2} \right] \alpha_1 & \left[\frac{\kappa}{\mu_1} + \frac{(l_2 + q_0)}{\mu_2} \right] \alpha_2 \\ \frac{\kappa}{\mu_1} + \frac{(l_1 - q_0)}{\mu_2} & \frac{\kappa}{\mu_1} + \frac{(l_2 - q_0)}{\mu_2} \end{bmatrix} \begin{bmatrix} b_{t1} \\ b_{t2} \end{bmatrix} = \begin{bmatrix} \frac{2\kappa a_i}{\mu_1} \\ \frac{2\kappa b_i}{\mu_1} \end{bmatrix} \quad (2.14)$$

and solved for using the inbuilt matlab function `linsolve` (see Appendix C at back). We could of course solve (2.14) analytically, but the solution is not especially illuminating and – especially when we add another set of boundary conditions for the finite crystal case – fairly inefficient.

For each value of ω , equation (2.14) can be solved and the reflection coefficient calculated from the formula

$$R = \frac{\bar{E}_r^2}{\bar{E}_i^2} = \frac{|E_{xr}|^2 + |E_{yr}|^2}{|E_{xi}|^2 + |E_{yi}|^2} \quad (2.15)$$

where E_z and E_y are given by the transformations (1.8). These values can then be plotted against ω .

For the following graphs the values $\epsilon_1 = 3$, $\epsilon_2 = 2.95$ and $q_0 = 5$ are used. For these values the frequency gap extends from roughly 8.66×10^8 to 8.74×10^8 Hz. Sending in right circularly polarized light or initial values $a_i = 1$ and $b_i = 0$ yields Figure 2.1 below. (Again see Appendix C for programming details).

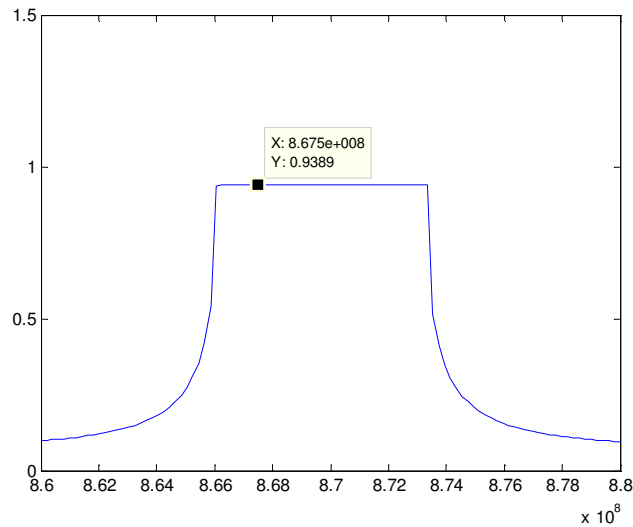


Figure 2.1

Plot of R vs. ω for $a_i = 1$ and $b_i = 0$. It can be seen R reaches roughly 0.94 in the gap.

This figure agrees nicely with de Gennes' predictions (6.1.4.7) for the regime of possible Bragg reflections. In the gap, the two modes in the liquid crystal are an approximately circular mode ($b_{t1} \gg a_{t1}$, approximately left circularly polarized) and a decaying mode with the decay constant of ℓ_2 . Since we send in light of the opposite polarization we would expect (as illustrated by de Gennes fig. 6.2) that the light in the gap is mostly reflected and that this light is right circularly polarized.

Why the reflectivity does not go perfectly to 1 is probably attributable to the fact that a_{t1} is still non-zero. The plateau shape of this figure tells us that whatever component

of the incident field had been transmitted in the form of the second travelling mode has gone to zero (because that mode decays in the gap).²

Below are plots for $a_i = 1$, $b_i = 1$ (Figure 2.2a) and $a_i = -1$, $b_i = 1$ (Figure 2.2b), linearly polarized light along the extraordinary and ordinary axes respectively. On the edges of the gap region (the real solutions of $\omega(0)$, ω_+ and ω_-) the cholesteric acts as a linear wave guide for linearly polarized light along the extraordinary axis at ω_- and the ordinary axis at ω_+ . Thus as we would expect, there is a large reflection coefficient at one edge of the gap (where the polarization of the incident light – perfectly right or left circular in xy space – matches that of the transmitted wave) linear and a much smaller amount of reflection at the opposite edge.

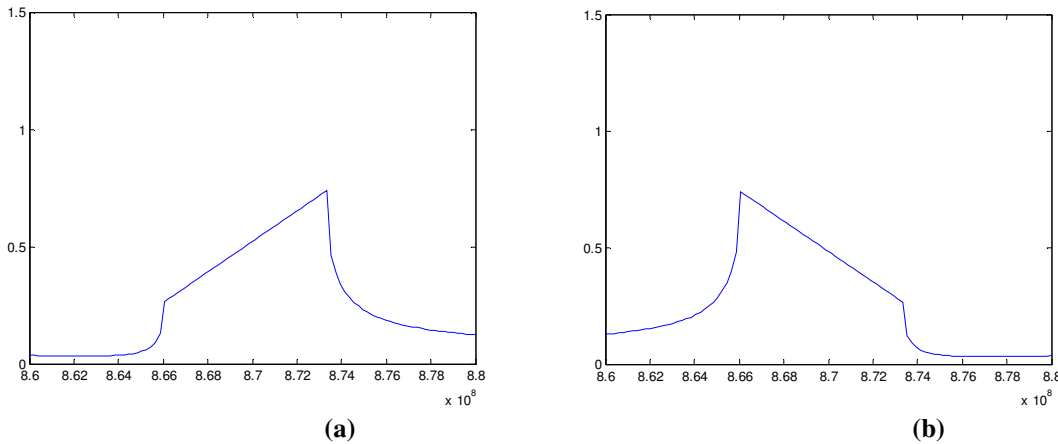


Figure 2.2: Plots of R vs. ω for (a) $a_i = 1$ and $b_i = 1$ and (b) $a_i = -1$ and $b_i = 1$.

Figure 2.3 below for incident light that is left circularly polarize ($a_i = 0$, $b_i = 1$) is not especially interesting except insofar as there is still a small amount of reflection pointing to the only approximate nature of de Gennes' results.

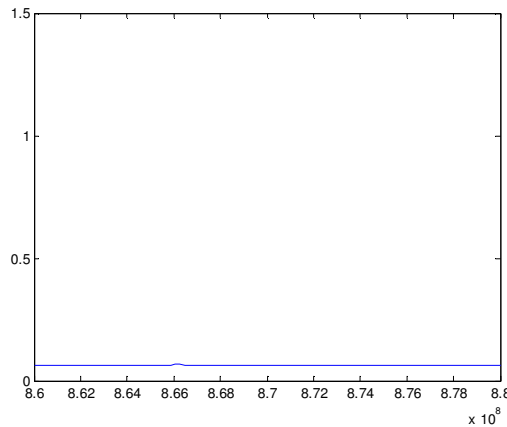


Figure 2.3
Plot of R vs. ω for $a_i = 0$ and $b_i = 1$.

² Ideally we would show that $R+T=1$ to check that the program was running correctly. I was not able to do this for the case of an infinite crystal, though for the finite crystal, this was always true (so that program appeared to be working). The difficulty arose in trying to figure out the transmission coefficient within the crystal. For the finite crystal figuring this out was not necessary.

For a finite crystal, the boundary condition problem is significantly more complicated. We must introduce a left traveling wave within the crystal which will have the ℓ -values corresponding to $d\omega/d\ell < 0$ outside the gap and the negative imaginary solution within the gap, or just $\ell_3 = -\ell_1$ and $\ell_4 = -\ell_2$. We must also introduce a transmitted wave after the second boundary which will look very similar to the incident wave (6) above (if the medium before the crystal is the same as that after). (Here there are 12 unknowns and as many equations that can be simplified to five by steps similar to those above. The resultant matrix is used in the program of Appendix D).

The most noticeable effect of making the crystal finite is that it introduces interference effects, that is, at certain frequencies the traveling modes within the crystal will add constructively or destructively and the reflection graph will oscillate outside the gap. Because a non-zero amount of the decaying wave can be transmitted across a finite crystal, however, there is also a somewhat observable rounding of the plateau shape from Figure 2.1. This is because at the edges of the band gap the decay constant is smaller than at the middle and the decaying mode transmits more energy. Figures 2.4a and 2.4b below display this trend.

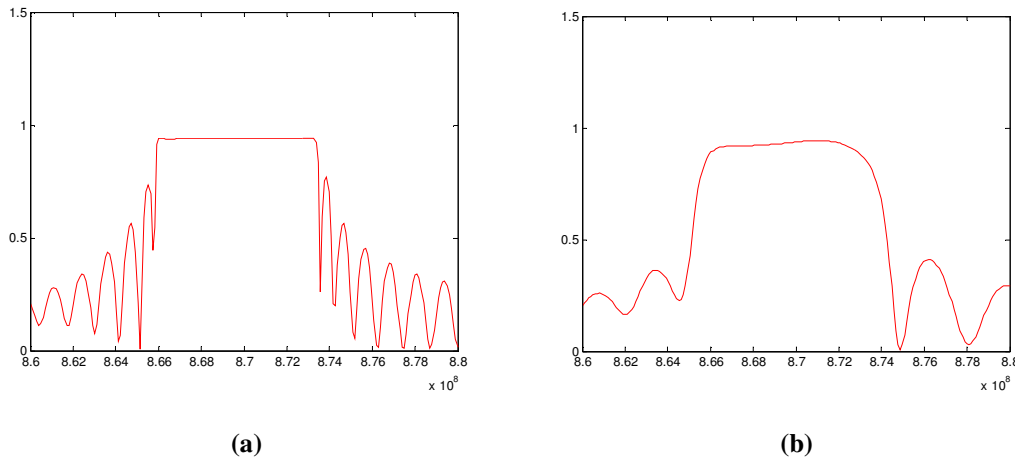


Figure 2.4: Plots of R vs. ω for $a_i = 1$ and $b_i = 0$ and crystal lengths (a) $d = 400$ and (b) $d = 150$

As the crystal depth becomes longer than the coherence length of the incident light, we expect not to see the oscillations outside the frequency gap anymore and the solutions will resemble those from the infinite crystal case more closely. Figure 2.5 below shows linearly polarized light incident upon a finite crystal.

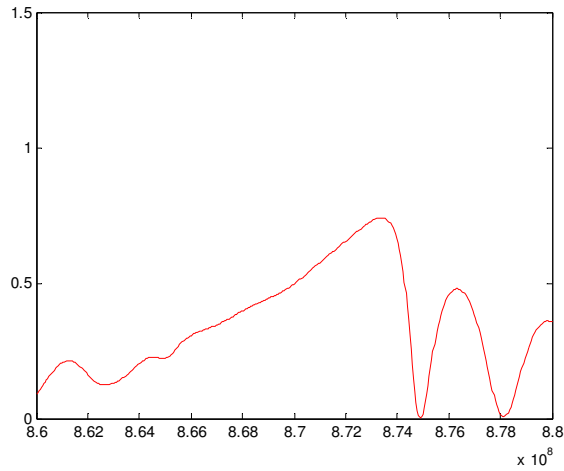
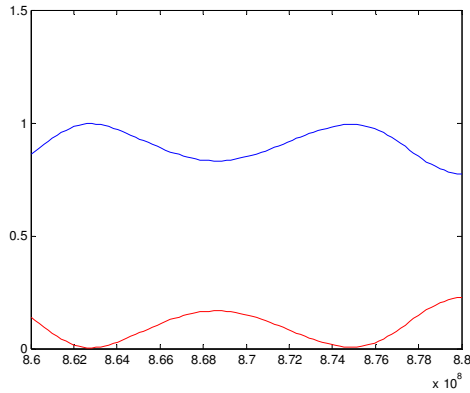
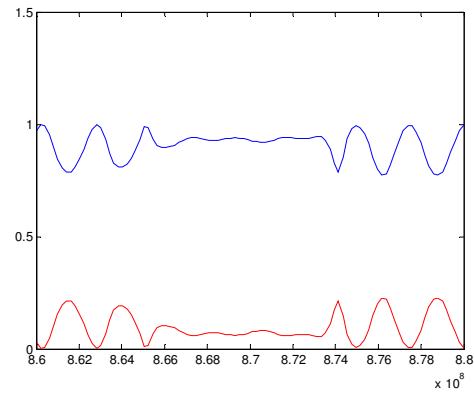


Figure 2.5
Plot of R vs. ω for $a_i = 1$ and $b_i = 1$ and crystal length $d = 200$

These final figures display both reflection (red) and transmission (blue) coefficients for a few crystal lengths with incident left circularly polarized light.



(a)



(b)

Figure 2.6: Plots of R vs. ω for $a_i = 0$ and $b_i = 1$ and crystal lengths (a) $d = 50$ and (b) $d = 150$

Section 3:

The special cases of finite and infinite crystals of constant pitch can provide some insight onto cases where the pitch varies as a function of z . Solving numerically for these cases turns out to be tricky. Warner and Kutter provide a nice alternative solution of the wave equation in a cholesteric, equation (3), by rotating into the frame of the director (this provides a solution in terms of the electric field along the director E_η and orthogonal to

the director E_ξ). The time independent wave equation (where, again, we have assumed a time dependence proportional to $e^{-i\omega t}$) is then given by

$$k_0^2 \epsilon_1 E_\xi = -E_\xi'' + E_\xi \phi'^2 + 2E_\eta' \phi' + E_\eta \phi'' \quad (3.1a)$$

$$k_0^2 \epsilon_2 E_\eta = -E_\eta'' + E_\eta \phi'^2 - 2E_\xi' \phi' - E_\xi \phi'' \quad (3.1b)$$

Where here, $k_0 = \omega/c$. (See Warner-Kutter for details). This pair of coupled second order differential equations can be rewritten as four first order equations. Letting $E_\xi = p$, $E_\eta = q$, $E_\xi' = m$ and $E_\eta' = n$ we have

$$m' = -k_0^2 \epsilon_1 p + p \phi'^2 + 2n \phi' + q \phi'' \quad (3.2)$$

$$n' = -k_0^2 \epsilon_2 q + q \phi'^2 - 2m \phi' - p \phi''$$

$$p' = m \quad \text{and} \quad q' = n$$

This allows matlab to solve numerically using the inbuilt function ode45. For the varying pitch case Warner and Kutter consider $\phi(z)$ is given by

$$\phi(z) = (q_0 + \frac{1}{2} \gamma q_0^2 z) z \quad (3.3)$$

Appendix E provides the matlab program for a numerical solution. Using that program we obtain Figure 3.1 which plots the electric field vs. z for a single frequency.

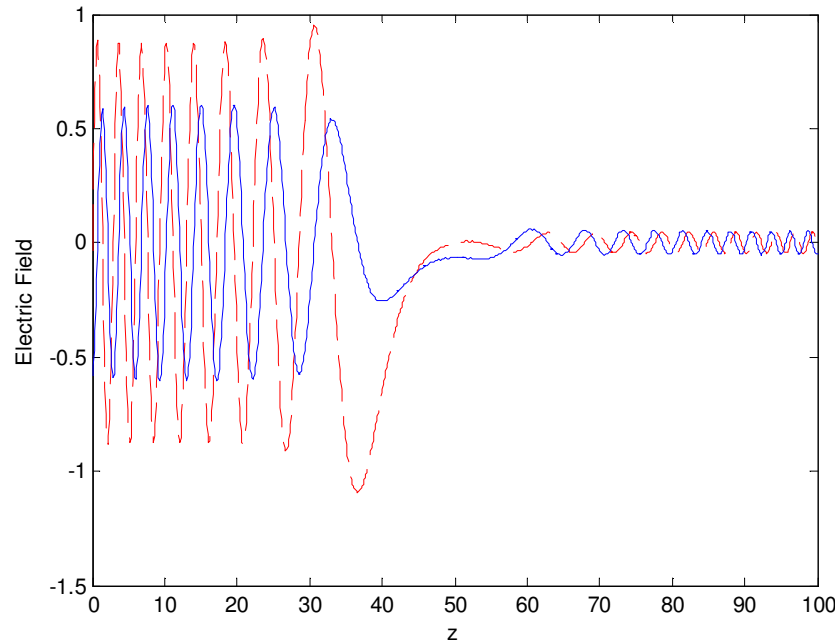


Figure 3.1
 E_ξ shown in red, E_η in blue. Graph is for initial values (@ $z=0$) $[m_0 \ n_0 \ p_0 \ q_0] = [2 \ -0.067 \ -0.036 \ -0.58]$

This figure shows us that across some critical range the pitch length will be such that the frequency of the incident light is in the gap. The wave decays across this critical region. Indeed the reflection coefficient behaves much like a step function (see Figure 3.2 below) for a certain polarization of incident light (right circular) and under the approximations made by de Gennes for circular regimes.

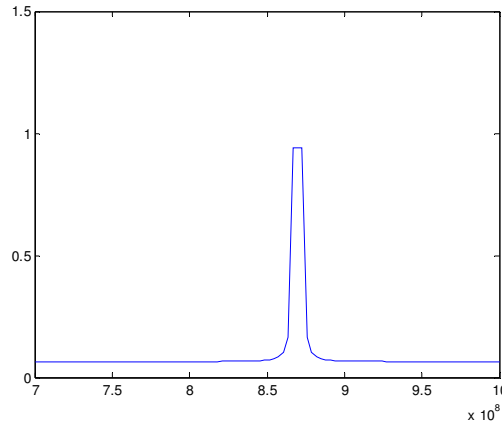


Figure 3.2
R vs. ω an expanded view of Figure 2.1

On these approximations it may be possible to treat the varying pitch case like a crystal of finite width equal to the width of this critical range.

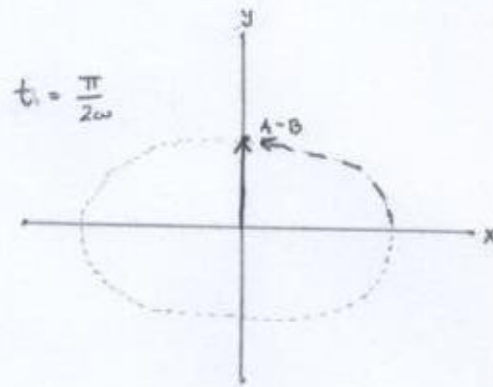
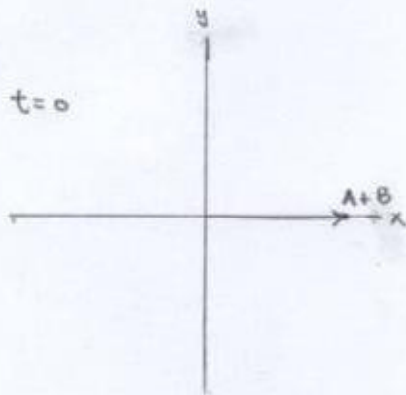
Obtaining exact numerical solutions for the reflection coefficient turns out not to follow in a straightforward manner from the type of program that made Figure 3.1 and the process used in Section 2. Previously, we were able to set up a boundary value problem because the electric field could be solved for analytically within the crystal. Now we must solve for the field numerically which introduces a new set of challenges. First, it seems to me that an infinite crystal of varying pitch will differ importantly from an infinite crystal of constant pitch in that we can no longer ignore the left traveling component within the crystal. A glance at Figure 3.1 tells us that it no longer makes sense to speak of *the* transmitted component (compare the amplitudes around $z = 10$ and $z = 90$). Rather a superposition of right and left traveling waves must account for this pattern. Second, the program that created Figure 3.1 requires that the user put in the initial values of the total field at the boundary. This introduces a second separation problem; we are no longer simply inputting the incident field value, but the total value of the field at the boundary – that is, the incident and reflected wave components.³

Somehow resolving this issue remains to be done before an analysis of light reflectivity off a varying pitch cholesteric yields testable results.

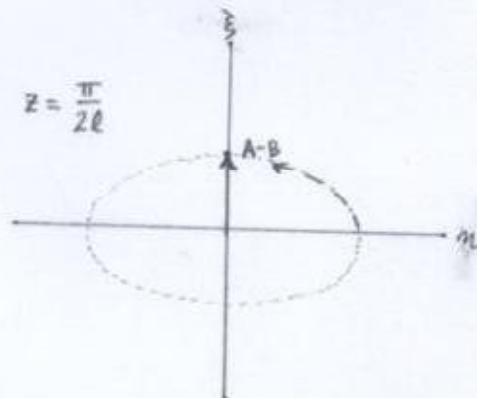
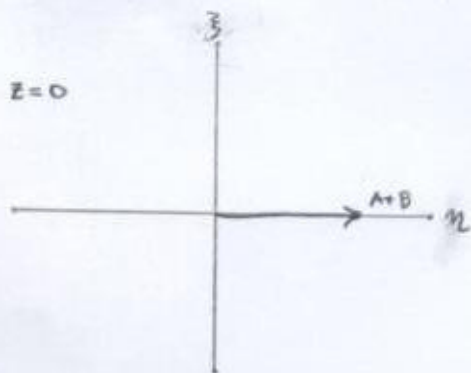
³This problem is related to the one mentioned in footnote number 2.

Appendix A

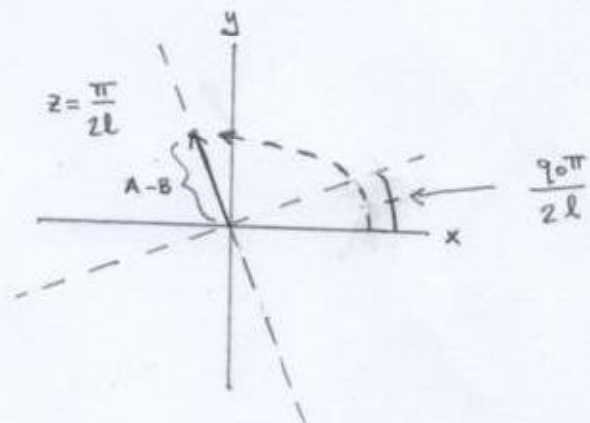
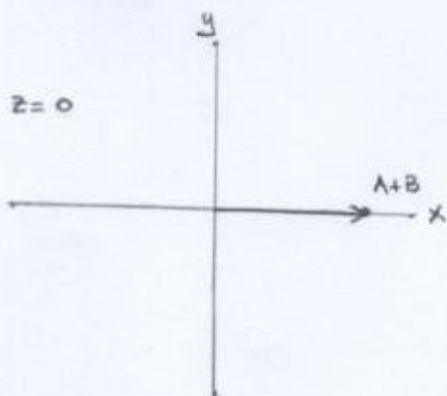
At $z = 0$:



At $t = 0$, rotated into director coordinate frame
(ξ - normal to director, η - parallel to director)



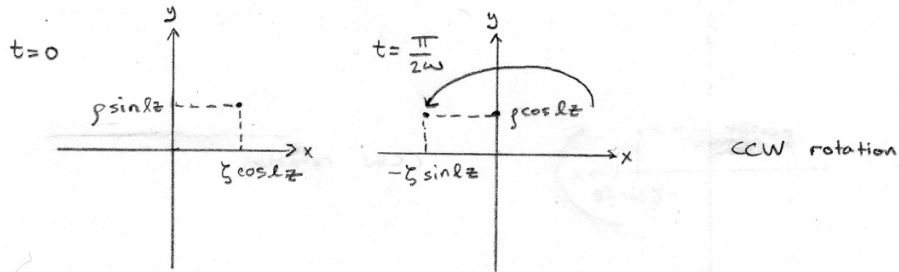
At $t = 0$, non-rotating frame (w/ director angle
changing linearly i.e. $\theta = q_0 z$)



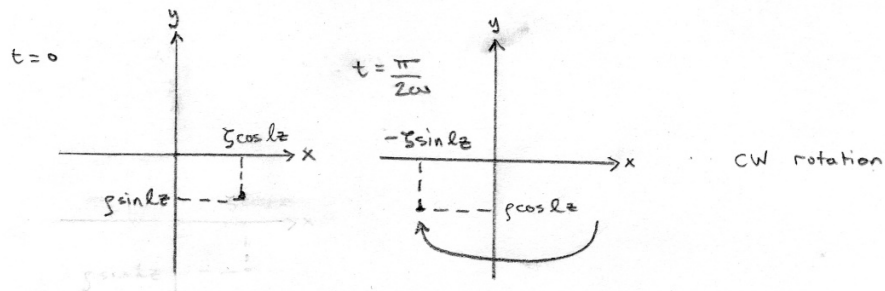
Appendix B

For the below figures a particular z (such that $0 < |z| < \pi/2$ and thus $\sin(|z|)$ & $\cos(|z|)$ are both greater than zero) has been chosen and we are observing the direction of rotation for various values of ℓ , ζ and ρ .

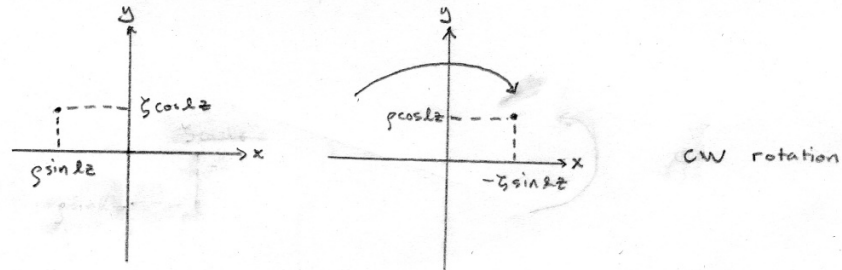
$$\ell > 0, \zeta > 0, \rho > 0$$



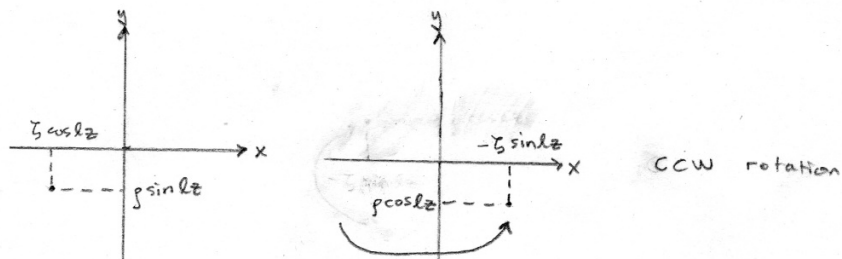
$$\ell > 0, \zeta > 0, \rho < 0$$

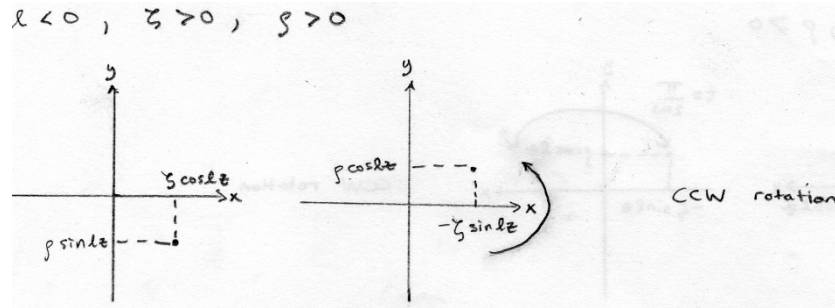


$$\ell > 0, \zeta < 0, \rho > 0$$



$$\ell > 0, \zeta < 0, \rho < 0$$





It can be seen that if $\rho/\zeta > 0$, then the field rotates counterclockwise and if $\rho/\zeta < 0$, it rotates clockwise. We leave it to the curious reader to check that this relation holds for the remaining three possible cases where $l < 0$ and for any set of cases assessed at a different z value.

Appendix C

In this appendix alone, I will try to illuminate some of the programming steps. The program in Appendix B is just a slightly more complicated version of this one. Descriptions are in bold, program text is in normal and colored font.

Infinite Crystal

Set out a list of constants.

```
c = 3E8;
e1 = 3;
e2 = 2.95;
q0 = 5;
m1 = 4*pi*1E-7;
m2 = 4.1*pi*1E-7;
```

Solve for the critical values of w (frequency) which define the gap region first symbolically, then evaluate them using the above constants.

```
wcrit = solve('(-(wc/c)^2*(e1 + e2)/2) + q0^2)^2 - ((wc/c)^2*(e1 - e2)/2)^2 = 0', 'wc');
wc = eval(wcrit);
```

Decide on the number of steps for the "for" loop below and create a frequency vector between values w_{min} and w_{max} with this many steps. This is essentially a measure of how precise you would like the following calculation to be or how many different values of w you would like to have a reflection coefficient for.

```
n = 100;
w = linspace(8.6E8, 8.8E8, n);
```

Begin "for" loop running from index $i = 1$ to $i = n$.

```
for i = 1:n
```

Define k_0^2 , k_1^2 and $k_n = \kappa$ (in the text above).

```
k0s(i) = (w(i)/c)^2*(e1 + e2)/2;
k1s(i) = (w(i)/c)^2*(e1 - e2)/2;
kn = 2*pi/(c/(w(i)));
```

Solve symbolically for l , this is from equation 6.24 in de Gennes, this will return a column vector with components l_1 , $-l_1$, l_2 , $-l_2$ from the above text.

```
l = solve('(-k0s(i) + l^2 + q0^2)^2 - 4*q0^2*l^2 - k1s(i)^2 = 0', 'l');
```

The first right traveling mode always corresponds to the l_d solution (evaluate this expression using the above constants). The second right traveling mode corresponds to the l_b solution before the gap and the l_c solution after the gap (where $dw/dl > 0$). Within the gap, the positive imaginary solution (which has the same place in the vector returned by this program as l_c) gives the correct decaying wave. The expression below gives a conditional statement for the value of l_2 which accounts for these different values.

```
l1 = eval(l(1));
if w(i) >= wc(1)
    l2 = eval(l(3));
else
    l2 = eval(l(4));
end
```

For symbolic efficiency we relate the transmitted components by constants α_1 and α_2 . See (11a) and (11b) above.

```
alpha1(i) = k1s(i)/((l1+q0)^2 - k0s(i));
alpha2(i) = k1s(i)/((l2+q0)^2 - k0s(i));
```

Define our incident amplitudes, in this case right circularly polarized light.

```
ai = 1;
bi = 0;
```

The reduced matrix below is a simplification of equations (9)-(11). These have been reduced to two equations involving unknowns bt_1 and bt_2 expressed in the form $\hat{A}\vec{b}_t = \hat{B}$ then solved for using the inbuilt matlab function `linsolve`.

```
A = [(kn/m1 + (l1+q0)/m2)*alpha1(i) , (kn/m1 + (l2+q0)/m2)*alpha2(i);
      kn/m1 + (l1-q0)/m2, kn/m1 + (l2-q0)/m2];

B = [2*kn*ai/m1; 2*kn*bi/m1];
bt = linsolve(A, B);
```

From this solution, the rest of the amplitudes from (9)-(11) can be determined.

```

ar(i) = alpha1(i)*bt(1) + alpha2(i)*bt(2) - ai;
at1(i) = alpha1(i)*bt(1);
at2(i) = alpha2(i)*bt(2);
br(i) = bt(1) + bt(2) - bi;

bt1(i) = bt(1);
bt2(i) = bt(2);

```

We may then convert these back to an xy coordinate plane and solve for the reflection coefficient. We then close the loop and plot R vs. w.

```

Eix = (ai + bi)/2;
Eiy = (ai - bi)/(2*1j);
Erx = (ar(i) + br(i))/2;
Ery = (ar(i) - br(i))/(2*1j);
R(i) = ((abs(Erx))^2 + (abs(Ery))^2)/((abs(Eix))^2 + (abs(Eiy))^2);
end

plot(w, R, '-')
axis([8.6E8 8.8E8 0 1.5])

```

Appendix D

Finite Crystal

```

c = 3E8;
e1 = 3;
e2 = 2.95;
q0 = 5;
m1 = 4*pi*1E-7;
m2 = 4.1*pi*1E-7;
wcrit = solve('(-(wc/c)^2*(e1 + e2)/2) + q0^2)^2 - ((wc/c)^2*(e1 - e2)/2)^2 = 0', 'wc');
wc = eval(wcrit);
d = 200;

n = 200;
w = linspace(8.4E8, 9E8, n);

for i = 1:n

k0s(i) = (w(i)/c)^2*(e1 + e2)/2;
k1s(i) = (w(i)/c)^2*(e1 - e2)/2;
kn = 2*pi/(c/(w(i)));
l = solve('(-k0s(i) + l^2 + q0^2)^2 - 4*q0^2*l^2 - k1s(i)^2 = 0', 'l');

l1 = eval(l(1));
if w(i) >= wc(1)
    l2 = eval(l(3));

```

```

else
    l2 = eval(l(4));
end
l3 = eval(l(2));
if w(i) <= wc(1)
    l4 = eval(l(3));
else
    l4 = eval(l(4));
end

alpha1 = k1s(i)/((l1+q0)^2 - k0s(i));
alpha2 = k1s(i)/((l2+q0)^2 - k0s(i));
alpha3 = k1s(i)/((l3+q0)^2 - k0s(i));
alpha4 = k1s(i)/((l4+q0)^2 - k0s(i));

beta1 = exp(1j*(l1+q0)*d);
beta2 = exp(1j*(l2+q0)*d);
beta3 = exp(1j*(l3+q0)*d);
beta4 = exp(1j*(l4+q0)*d);
beta5 = exp(1j*(l1-q0)*d);
beta6 = exp(1j*(l2-q0)*d);
beta7 = exp(1j*(l3-q0)*d);
beta8 = exp(1j*(l4-q0)*d);

ai = 0;
bi = 1;

A = [(kn/m1 + (l1+q0)/m2)*alpha1, (kn/m1 + (l2+q0)/m2)*alpha2, ((kn/m1
+ (l3+q0)/m2)*alpha3), ((kn/m1 + (l4+q0)/m2)*alpha4), 0, 0;
    kn/m1 + (l1-q0)/m2, kn/m1 + (l2-q0)/m2, kn/m1 + (l3-q0)/m2, kn/m1
+ (l4-q0)/m2, 0, 0;
    alpha1*beta1, alpha2*beta2, alpha3*beta3, alpha4*beta4, -
exp(1j*kn*d), 0;
    beta5, beta6, beta7, beta8, 0, -exp(1j*kn*d);
    ((l1+q0)/m2)*beta1*alpha1, ((l2+q0)/m2)*beta2*alpha2,
((l3+q0)/m2)*beta3*alpha3, ((l4+q0)/m2)*beta4*alpha4, -
(kn/m1)*exp(1j*kn*d), 0;
    ((l1-q0)/m2)*beta5, ((l2-q0)/m2)*beta6, ((l3-q0)/m2)*beta7, ((l4-
q0)/m2)*beta8, 0, -(kn/m1)*exp(1j*kn*d)];

B = [2*kn*ai/m1; 2*kn*bi/m1; 0; 0; 0; 0];
x = linsolve(A, B);

ar(i) = alpha1*x(1) + alpha2*x(2) + alpha3*x(3) + alpha4*x(4) - ai;
acr1(i) = alpha1*x(1);
acr2(i) = alpha2*x(2);
acl1(i) = alpha3*x(3);
acl2(i) = alpha4*x(4);
at(i) = x(5);

br(i) = x(1) + x(2) + x(3) + x(4) - bi;
bcr1(i) = x(1);
bcr2(i) = x(2);
bcl1(i) = x(3);

```



```

bcl2(i) = x(4);
bt(i) = x(6);

Eix = (ai + bi)/2;
Eiy = (ai - bi)/(2*1j);
Erx = (ar(i) + br(i))/2;
Ery = (ar(i) - br(i))/(2*1j);
Etx = (at(i) + bt(i))/2;
Ety = (at(i) - bt(i))/(2*1j);
R(i) = ((abs(Erx))^2 + (abs(Ery))^2)/((abs(Eix))^2 + (abs(Eiy))^2);
T(i) = ((abs(Etx))^2 + (abs(Ety))^2)/((abs(Eix))^2 + (abs(Eiy))^2);

end

plot(w, R, 'r-', w, T, 'b-')
axis([8.4E8 9E8 0 1.5])

```

Appendix E

The file below creates a function “bragg” to be called by the second program. This function should be saved as bragg.m.

```

function mprime = bragg(z, m)

%define constants
k0 = 2;
e1 = 2.25;
e2 = 3.24;
g = 1;
h = 0.05;

a = (g + 0.5*h*g^2*z)*z;
da = g + h*g^2*z;
dda = h*g^2;

%create column vector of 4 first order derivatives for the E-field, m,
%with respect to z.
mprime(1) = -k0^2*e1*m(3) + m(3)*da^2 + 2*m(2)*da + m(4)*dda;
mprime(2) = -k0^2*e2*m(4) + m(4)*da^2 - 2*m(1)*da - m(3)*dda;
mprime(3) = m(1);
mprime(4) = m(2);
%ensure mprime is a column vector
mprime = mprime(:);

```

This second program defines a range for which to evaluate the function above and the desired number of solutions or accuracy. It uses the inbuilt matlab function ode45 to solve it.

```
z0 = 0; %starting z
zf = 40; %ending z
nsteps = 1000; %number of steps
zspan = linspace(z0, zf, nsteps);
m0 = [2 -0.067 -0.036 -0.58]; %initial field and field derivative
values

%solve differential equations
[z, s] = ode45(@bragg, zspan, m0);
m = s(:, 1);
n = s(:, 2);
p = s(:, 3);
q = s(:, 4);

plot(z, p, '--r', z, q, '-b')
xlabel('z')
ylabel('Electric Field')
```